

Mechanism Analysis and Behavior Characterization of Stick-Slip Vibration

Zhiqiang Wang^{1,2} and Zhenyu Lei²

¹ Shijiazhuang Tiedao University, State Key Laboratory of Mechanical Behavior and System Safety of Traffic Engineering Structures, 050043 Shijiazhuang, China, wangzq@tongji.edu.cn

² Shanghai Key Laboratory of Rail Infrastructure Durability and System Safety, 201804 Shanghai, China, 2010805@tongji.edu.cn

Abstract: In order to clarify stick-slip vibration mechanisms and characterize stick-slip vibration behaviors, a three-dimensional numerical model of the slider-plate friction contact was established using the finite element method, and the mechanism characteristics of slip vibration and stick-slip vibration were analyzed in terms of contact stick-slip and vibration responses. Meanwhile, the stick-slip vibration behaviors of the system under the influence of different parameters were investigated. The results show that depending on the vibration form of the system, the distribution and amplitude of contact stresses in adhesion and slip states differ. The frequency domain curve of the friction force for the slip vibration mainly includes three characteristic frequency ranges, namely, 0~75 Hz, 80~150 Hz and 1300~1600 Hz, while the characteristic frequency component of the friction force for the stick-slip vibration mainly exhibits 0~65 Hz. Therefore, the high-frequency component of the friction force may originate from the continuous slip vibration. The presence and monotonically increasing (or constant) of the relative velocity at the contact interface drives the formation of the slip vibration, while the presence of non-monotonically varying relative velocity drives the formation of the stick-slip vibration. Appropriate reductions in spring stiffness and plate motion velocity and increases in the damper damping will slow down the degree of stick-slip vibration, thereby reducing the effect of stick-slip vibration on the system behavior. In addition, compared to the constant value friction characteristic of the contact interface, the exponential decay friction characteristic has a smaller effect on the degree of stick-slip vibration of the system.

Keywords: stick-slip vibration; slip vibration; friction contact; relative velocity; mechanism property

1 Introduction

Friction usually results in wear and vibration at a contact interface, which in turn leads to manufacturing errors and noise pollution. The phenomenon of friction

vibration exists widely in people's daily lives and in various industrial fields, it has always been one of the hot issues that concerns tribology researchers [1-4]. Friction-induced vibration may adversely affect the normal performance of mechanical systems and has two main manifestations: stick-slip vibration and quasi-harmonic vibration [5] [6]. The stick-slip vibration exhibits a sawtooth displacement-time variation curve with well-defined adhesion and slip phases. In the adhesion phase, the stick-slip motion is governed by the static friction force; in the slip phase, the stick-slip motion is governed by the dynamic friction force associated with the slip velocity. The quasi-harmonic vibration exhibits an approximately sinusoidal displacement-time variation curve, and this motion is formed and maintained during the slip phase. The quasi-harmonic vibration is generally caused by peaks in the friction-velocity curve [5].

Friction force exhibits different characteristics at different phases. In the adhesion phase, friction force prevents the onset of motion of an object in equilibrium; in the slip phase, friction force prevents the existing form of motion of an object [7]. Since the dynamic and static friction coefficients are different and present non-smooth transitions, the motion of an object will also present non-smooth characteristics, therefore, the stick-slip system belongs to the non-smooth system [8]. In addition, some of the degrees of freedom in the stick-slip system are constrained during the adhesion phase, and thus the stick-slip system also belongs to the category of non-smooth systems with variable structures, i.e., the number of state variables of the system changes with time.

Stick-slip vibration occurs in many types of engineering systems and in everyday life, such as the sound of a bow-string violin, squeaky chalk and shoes, and railroad wheel-rail systems and brake-wheel systems with squealing, most of which are caused by the sliding friction at the contact interface. Some scholars have made an early start on the study of stick-slip vibration and have conducted relatively in-depth theoretical and experimental analysis [5]. Using the friction model, Popp and Rudolph [9] proposed three methods for controlling the stick-slip motion of the system, namely, increasing the internal damping of the system to compensate for the negative damping due to friction properties, applying external excitation to break the limit cycle, and passively controlling the system by means of the fluctuating normal force. Hong *et al.* [10] analyzed the stick-slip vibration between an axially flexible beam fixed at both ends and an oscillator, and the results showed that the long-period stick-slip vibration was mainly subject to the oscillator, while the short-period stick-slip vibration was mainly subject to the axial deformation of the beam. Meanwhile, Hong *et al.* [10] found that applying a high damping ratio to the oscillator did not suppress the stick-slip vibration induced due to the axial deformation of the beam. Maegawa *et al.* [11] investigated the effect of mass, stiffness and damping coefficient of the elastic foundation on the stick-slip occurrence or not based on the stick-slip model of a 2DOF system, and found that when the parameters of the elastic foundation were determined according to the optimal parameter tuning method of the dynamic

damper theory, the range of stick-slip occurrence was reduced in comparison with the slip system without the elastic foundation. Leus and Abrahamowicz [12] gave some experimental results on the stick-slip phenomenon using an indoor test bench. The analysis showed that longitudinal vibration could reduce or even completely eliminate the stick-slip phenomenon. Abdo and Zaier [13] designed and constructed a new test machine to investigate the effect of vibration amplitude and vibration frequency of the test specimen on the contact stick-slip amplitude. The results indicated that the stick-slip amplitude depended on the type of material and decreased with the increase of the vibration amplitude. Balaram et al. [14] investigated the suppression of stick-slip vibration in disc brakes by applying a normal harmonic force with a small amplitude on the brake pad, and determined the frequency range of the normal force to suppress the occurrence of stick-slip vibration. The results demonstrated that the onset and termination of the entrainment interval were associated with a Neimark-Sacker bifurcation, and that the transition-slip bifurcation occurring in the entrainment interval produced a subinterval associated with the suppression of stick-slip vibration. Dong et al. [15] examined friction vibration and noise during the stick-slip process of ceramic/metal friction, and found that the roughness peak at the contact interface induced vibration and noise during the slip phase, and that the main vibration frequency increased with the increase of slip velocity and external load. Zhou et al. [16] established the relationship between tangential load and tangential displacement for rough contact surfaces and analyzed the effect of system parameters on the energy dissipation. Qian et al. [17] studied the effect of normal/tangential damping on the stability of the system using a mathematical modeling approach, and found that an optimal damping ratio would exist for the system to make it the most stable. Wang et al. [18] analyzed the dynamical characteristics of a class of non-smooth systems containing the Dankowicz dynamic friction, and the results showed that there were various forms of stick-slip/chatter transition motions in the system. Song and Yan [19] elaborated the related research on the stick-slip friction from both macroscopic and microscopic scales, and analyzed the key issues in the research of interfacial stick-slip friction.

From the above literature investigation, it can be found that the existing research mainly utilizes the rigid body model to carry out analytical or numerical calculations in order to study the stick-slip phenomenon at the contact interface, and this method can effectively explain the characteristics of the stick-slip vibration mechanism. Unlike the above research method, this paper mainly employs the flexible body model to perform numerical simulations, thereby studying the contact stick-slip vibration mechanism and characterizing the stick-slip behavior. Compared with the rigid body model, the flexible body model can reflect the contact state in detail and consider the elastic deformation, which is of positive significance for the comprehensive understanding of the stick-slip phenomenon. Given that, with the help of the finite element software ABAQUS, this paper establishes a three-dimensional numerical model of slider-plate friction

contact, analyzes the vibration form and influence mechanism of the stick-slip phenomenon, and carries out a comparative study of the vibration behavior.

2 Numerical Model

Using the finite element software Abaqus, a three-dimensional model of slider-plate friction contact is established in this section, which includes a slider, a plate and a set of spring and damper. In the model, the contact interface between the slider and the plate adopts "hard" contact in the normal direction [20-23], and adopts the friction formula of static friction-dynamic friction exponential decay in the tangential direction, in which the coefficient of static friction is 0.35, the coefficient of dynamic friction is 0.25, the attenuation coefficient is 0.001 [24-28], and the tangential friction curve is shown in Fig. 1. The slider is located on the top of the plate, connected to the fixed point by a set of spring and damper, and its upper surface is subjected to a vertically downward normal compressive stress with an amplitude of 0.1 MPa. The diagram of the numerical model is shown in Fig. 2, and the model connection and material parameters are shown in Table 1. In the initial condition, the plate has a form of motion in the $-z$ direction as shown in Fig. 2.

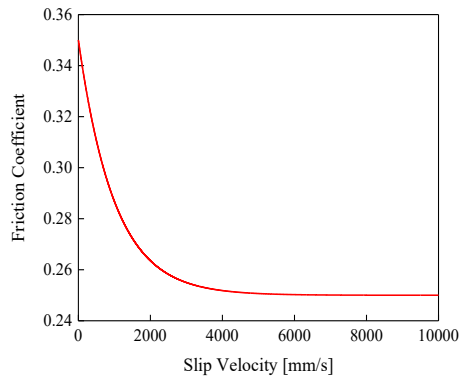


Figure 1

Tangential friction curve of the slider-plate contact

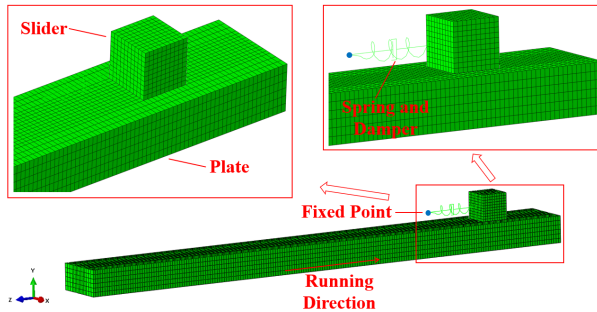


Figure 2

Numerical model of the slider-plate contact

Table 1
Model parameter values

Parameter		Value
normal compressive stress		0.1 MPa
spring stiffness		$10 \text{ N}\cdot\text{mm}^{-1}$
damper damping		$5 \text{ Ns}\cdot\text{mm}^{-1}$
friction coefficient		0.35 - 0.25 (0.001)
slider/plate material	density	$7800 \text{ kg}\cdot\text{m}^{-3}$
	elastic modulus	$2.1 \times 10^5 \text{ MPa}$
	Poisson's ratio	0.3
	yield stress	838 MPa

3 Analysis of Stick-Slip Vibration Mechanism - Slip Vibration

The plate is set to have a uniformly accelerated motion in the $-z$ direction, and the velocity loading amplitude curve is shown in Fig. 3, in which the loading interval is 1~5 s (0~1 s is the normal compressive stress loading interval). By performing numerical calculations, the mechanism characteristics of the stick-slip phenomenon are investigated in this section in terms of both contact stick-slip and vibration responses.

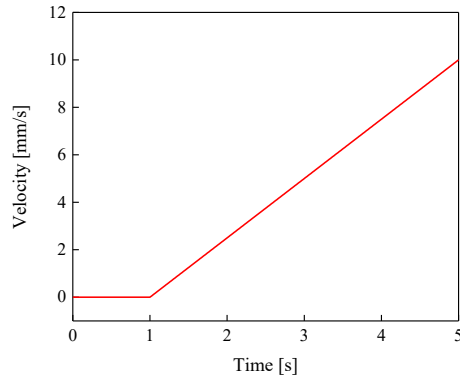


Figure 3

Amplitude curve of velocity loading

3.1 Contact Stick-Slip

Under the condition of the velocity loading amplitude curve shown in Fig. 3, the variation of the contact stick-slip state obtained from the simulation of the flexible body model is shown in Fig. 4. The contact stick-slip states at 5 representative moments are given in Fig. 4, characterizing the behavior change (stick/slip). From Fig. 4, it can be obtained that the contact state gradually transitions from the adhesion to the slip with the increase of the plate motion velocity, indicating that the contact interface undergoes stick-slip motion at this time. Since the plate motion velocity shows a linear increase, the contact interface will continue to maintain the slip motion after entering the slip state.

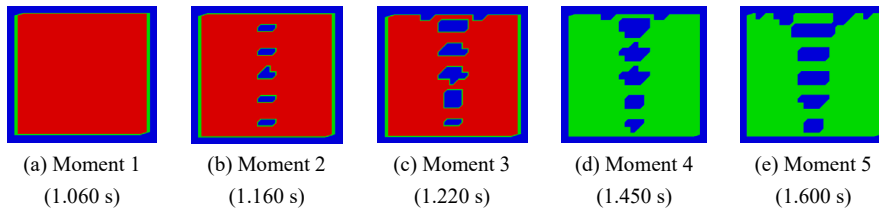


Figure 4

Contact stick-slip states with the plate velocity considered (red indicates adhesion, green indicates slip, blue indicates no contact)

The contact stresses in the adhesion and slip states corresponding to moments 1 and 5, which are only obtainable in the flexible body model, are shown in Figs. 5~6, where Fig. 5 shows the normal contact stresses and Fig. 6 shows the tangential contact stresses. From Fig. 5, it can be seen that the distribution of normal contact stresses in the adhesion and slip phases have different forms, and

the maximum value of normal contact stress corresponding to the slip phase (0.5891 MPa) is larger than that corresponding to the adhesion phase (0.1806 MPa), with the former being about 3.2619 times that of the latter. Similarly, from Fig. 6, it can be seen that the distribution of tangential contact stresses in the adhesion and slip phases are also different, and the maximum tangential contact stress in the slip phase (0.0381 MPa) is significantly larger than that in the adhesion phase (0.0002 MPa), which is about 190.5 times that of the latter.

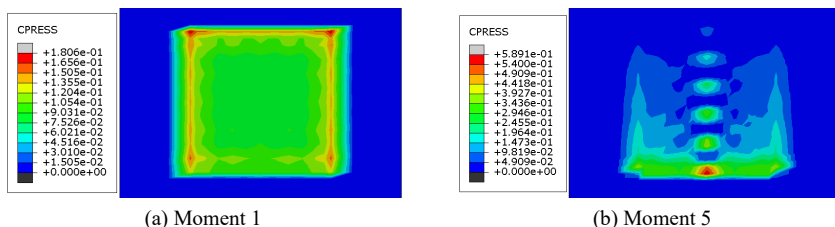


Figure 5

Normal contact stresses with the plate velocity considered

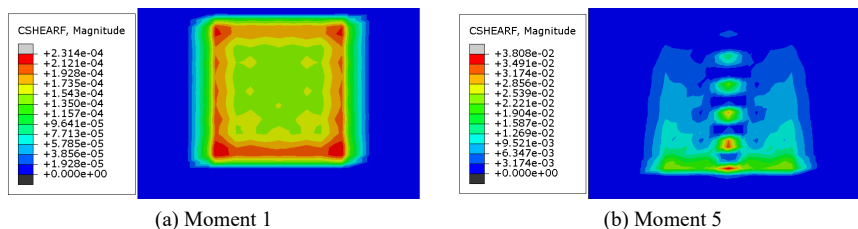


Figure 6

Tangential contact stresses with the plate velocity considered

3.2 Vibration Responses

During the motion process of the plate, the friction force variation curve of the slider-plate contact interface is shown in Fig. 7. From Fig. 7(a), it can be obtained that the vibration degree of the friction force increases gradually with the increase of the plate motion velocity. Meanwhile, according to Fig. 7(a), it can be seen that the duration of the adhesion phase is about 0.225 s (red curve in Fig. 7(a)), and it is followed by the slip phase (blue curve in Fig. 7(a)). Therefore, specifically, the process consists of one stick-slip vibration and multiple slip vibrations, i.e., the process reflects more the slip vibration characteristics of the slider-plate friction contact system. By performing Fast Fourier Transform (FFT) on the time domain curve of the friction force shown in Fig. 7(a), the corresponding frequency domain curve of the friction force can be obtained as shown in Fig. 7(b). From Fig. 7(b), it can be seen that the characteristic frequency components of the friction force are more complex, mainly including three frequency ranges of 0~75 Hz, 80~150 Hz

and 1300~1600 Hz, which are related to the natural properties of the slider-plate friction contact system.

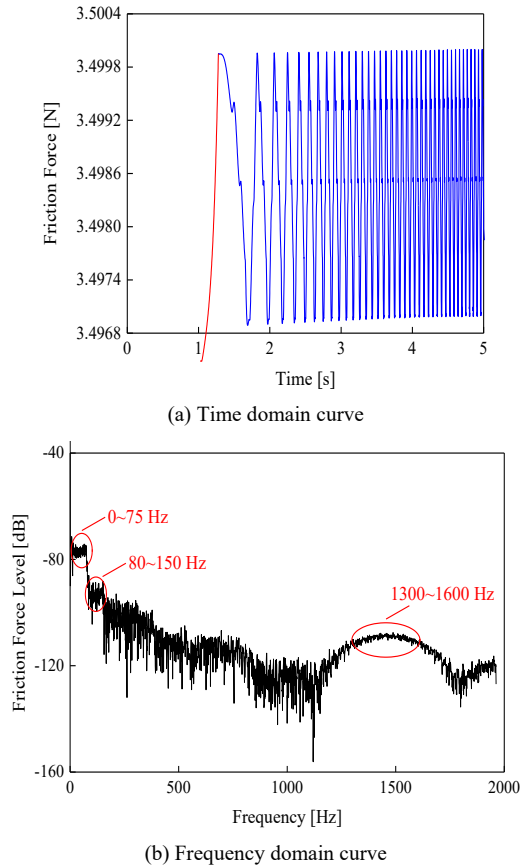


Figure 7

Friction force curves with the plate velocity considered

Further, the displacement response curves of the slider during the above process are extracted in this section, as shown in Fig. 8. From Fig. 8(c), it can be seen that the slider has been in a unidirectional (longitudinal $-z$) motion state, and the longitudinal displacement increases at a gradually decreasing rate, indicating that the slider gradually transitions from the initial static adhesion phase to the dynamic slip phase. Figure 8(a) and (c), on the other hand, reflect the vibration response characteristics of the slider in both transverse and vertical directions, in which the amplitude of the transverse displacement variation is relatively small, and the vertical displacement vibration characteristics are similar to the friction force vibration characteristics shown in Fig. 7(a).

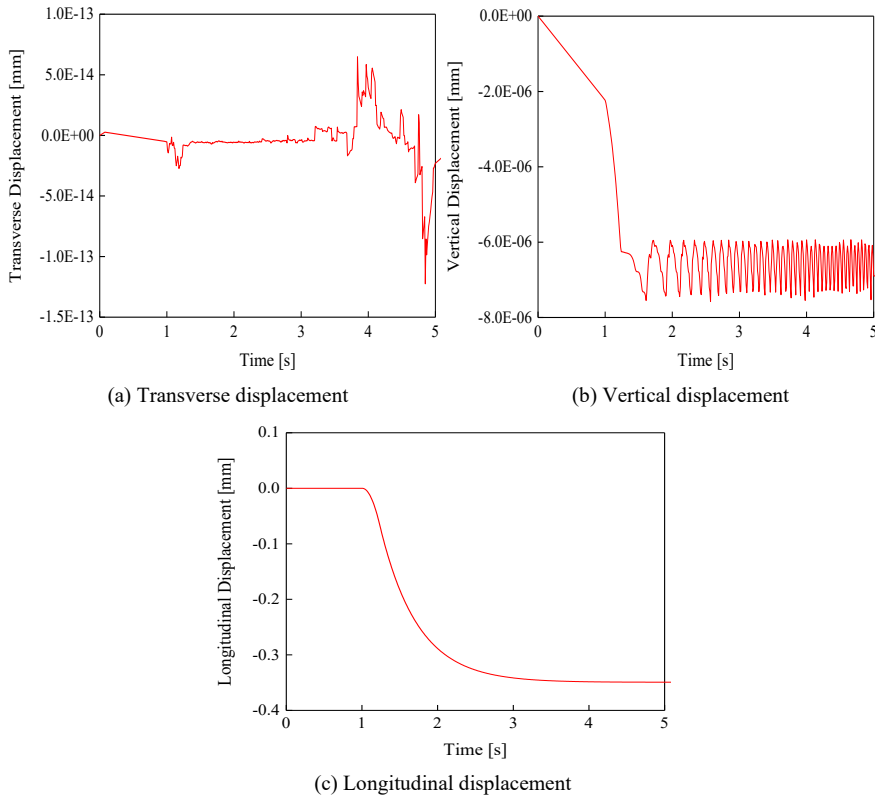


Figure 8

Response curves of slider displacements with the plate velocity considered

Combining Figs. 7~8, it can be found that the direct cause of the transformation of the slider-plate friction contact system from the stick-slip vibration to the slip vibration is the increase of the plate velocity. In this process, the longitudinal velocity of the slider shows that it increases first (adhesion phase) and then decreases (slip phase), and eventually tends to 0 (at this time, the spring/damping force and the friction force of the slider tends to be balanced), as shown in Fig. 9 (red curve). Meanwhile, according to Fig. 3 and Fig. 7(a), the critical value of the velocity for the occurrence of the above transition can be calculated as 0.5625 mm/s ($0.225 \times 10/4$). The occurrence of the slip vibration indicates that the contact interface undergoes the relative slip, i.e., there exists a relative velocity at the contact interface, as shown in Fig. 5 (blue curve), and it is easy to find that the interface relative velocity curve shows a monotonically increasing trend in the slip phase. Consequently, the occurrence mechanism of the slip vibration can be described as the presence and monotonically increase (or constancy) of the relative velocity at the contact interface induces the formation of the slip vibration.

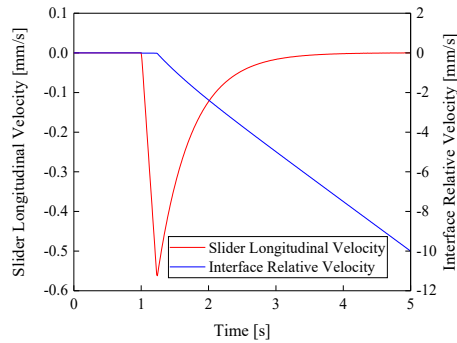


Figure 9

Velocity curves with the plate velocity considered

4 Analysis of Stick-Slip Vibration Mechanism - Stick-Slip Vibration

The formation mechanism of the slip vibration is mainly analyzed in Section 3, on the basis of which the occurrence mechanism of the sustained stick-slip vibration will be analyzed in this section. Since the successive transitions of the adhesion and slip states inevitably involve an “increase-decrease” cycle in the velocity of the slider motion, therefore, the boundary and loading conditions of the numerical model are adjusted in this section as follows: The velocity loading of the plate is canceled and the bottom surface of the plate is fully restrained; a longitudinal tensile stress is applied to one longitudinal end face of the slider, as shown in Fig. 10, and the variation curve of tensile stress amplitude is shown in Fig. 11; the other conditions are consistent with the numerical model in Section 2.

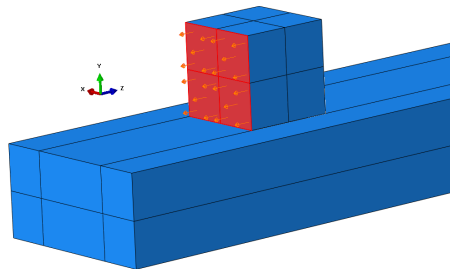


Figure 10

Diagram of longitudinal tensile stress application

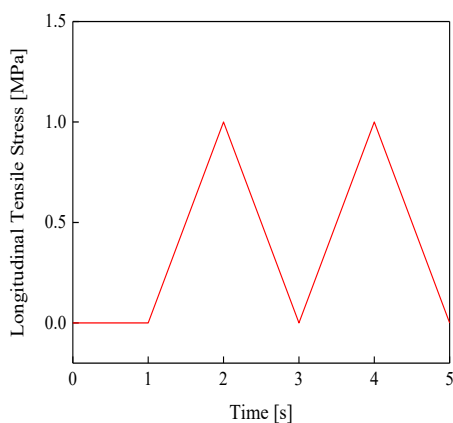


Figure 11

Amplitude curve of longitudinal tensile stress

4.1 Contact Stick-Slip

By numerical calculations, the stick-slip state diagram of the slider-plate contact interface can be attained as shown in Fig. 12. Figure 12 gives diagrams of contact stick-slip states at 10 representative moments, where moments 1, 4, 7 and 10 represent the adhesion state and moments 2, 3, 5, 6, 8 and 9 represent the slip state. Through the analysis, it can be reached that with the variation of longitudinal tensile stress amplitude, the contact state shows the phenomenon of adhesion-slip alternation, which indicates that the cyclic stick-slip motion occurs at the contact interface. Compared to the single stick-slip motion in the initial stage shown in Fig. 4, the stick-slip motion shown in Fig. 12 has a significant continuity.

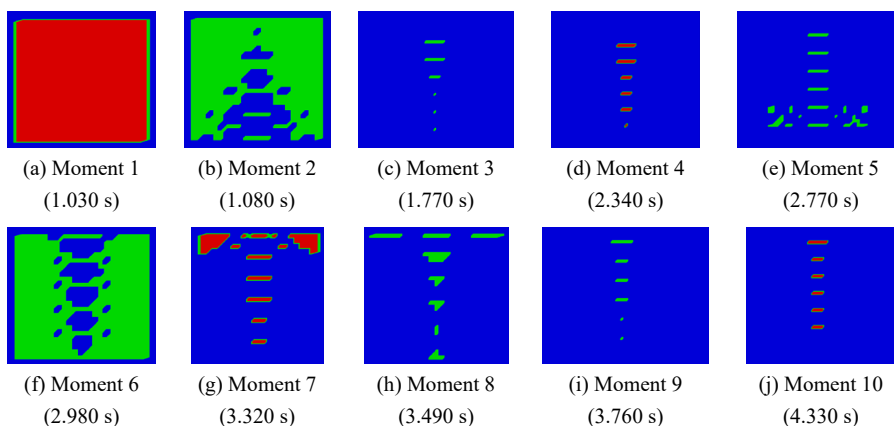


Figure 12

Contact stick-slip states with the slider longitudinal tensile stress considered (red indicates adhesion, green indicates slip, blue indicates no contact)

The contact stresses in the adhesion and slip states corresponding to moments 3 and 4 are shown in Figs. 13~14. For the normal contact stress, it can be seen from Fig. 13 that the stress maximum in the adhesion phase (4.505 MPa) is significantly larger than that in the slip phase (2.880 MPa), with the former being about 1.564 times larger than the latter. For the tangential contact stress, it can be obtained from Fig. 14 that the stress maximum in the adhesion phase (0.1013 MPa) is smaller than that in the slip phase (0.2520 MPa), and the former is about 40.1984% of the latter, which is closely related to the vibration form of the system.

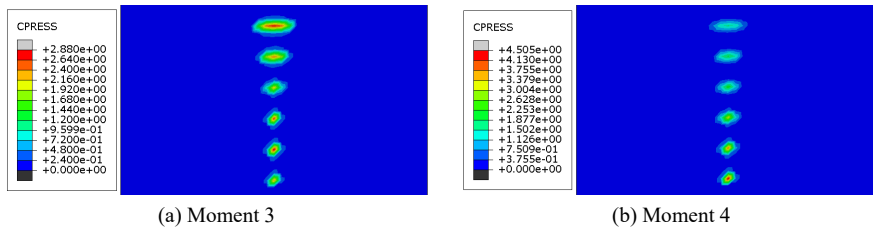


Figure 13

Normal contact stresses with the slider longitudinal tensile stress considered

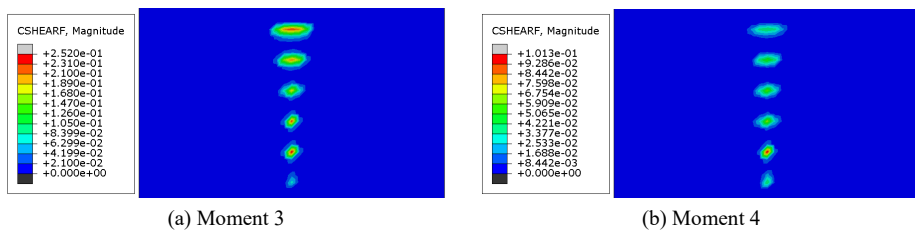


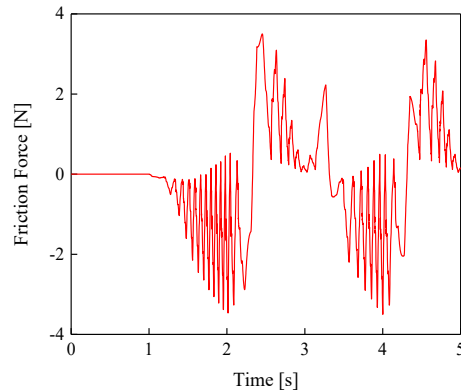
Figure 14

Tangential contact stresses with the slider longitudinal tensile stress considered

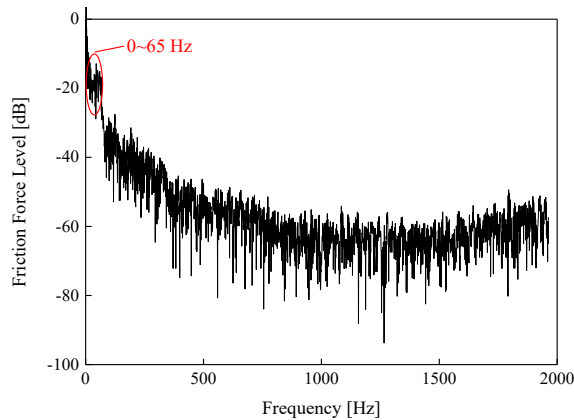
4.2 Vibration Responses

During the stick-slip vibration process described in Section 4.1, the friction force variation curve at the slider-plate contact interface is shown in Fig. 15. From Fig. 15(a), it can be seen that the friction force appears the vibration form with opposite directions as the amplitude of the longitudinal tensile stress varies, which reflects the alternating variation of the motion direction of the slider. Similarly, the FFT transform is performed on the friction force time domain curve shown in Fig. 15(a) and the corresponding friction force frequency domain curve can be obtained, as shown in Fig. 15(b). From Fig. 15(b), it can be seen that the characteristic frequency components of the friction force are still more complex, in which the main characteristic frequency component is 0~65 Hz. In addition, unlike the frequency domain curve of the friction force for the slip vibration (Fig. 7(b)), the frequency domain curve of the friction force for the stick-slip vibration (Fig. 15(b)) does not show the high-frequency component, which suggests that the

high-frequency component of the friction force may be related to the sustained slip vibration.



(a) Time domain curve



(b) Frequency domain curve

Figure 15

Friction force curves with the slider longitudinal tensile stress considered

Meanwhile, the displacement response curves of the slider during the above process are given in this section, as shown in Fig. 16. From Fig. 16(c), it can be seen that the slider is in a bi-directional (longitudinal $-z$ and z) motion state, i.e., the velocity of the slider is presented as an increasing-decreasing reciprocating cycle, which ensures the occurrence possibility of the stick-slip vibration. Figure 16(a) and (c) characterize the vibration responses of the slider in both transverse and vertical directions, where the transverse displacement varies with the same relatively small amplitude, and the vertical displacement has a vibration tendency similar to the amplitude of the friction force shown in Fig. 15(a).

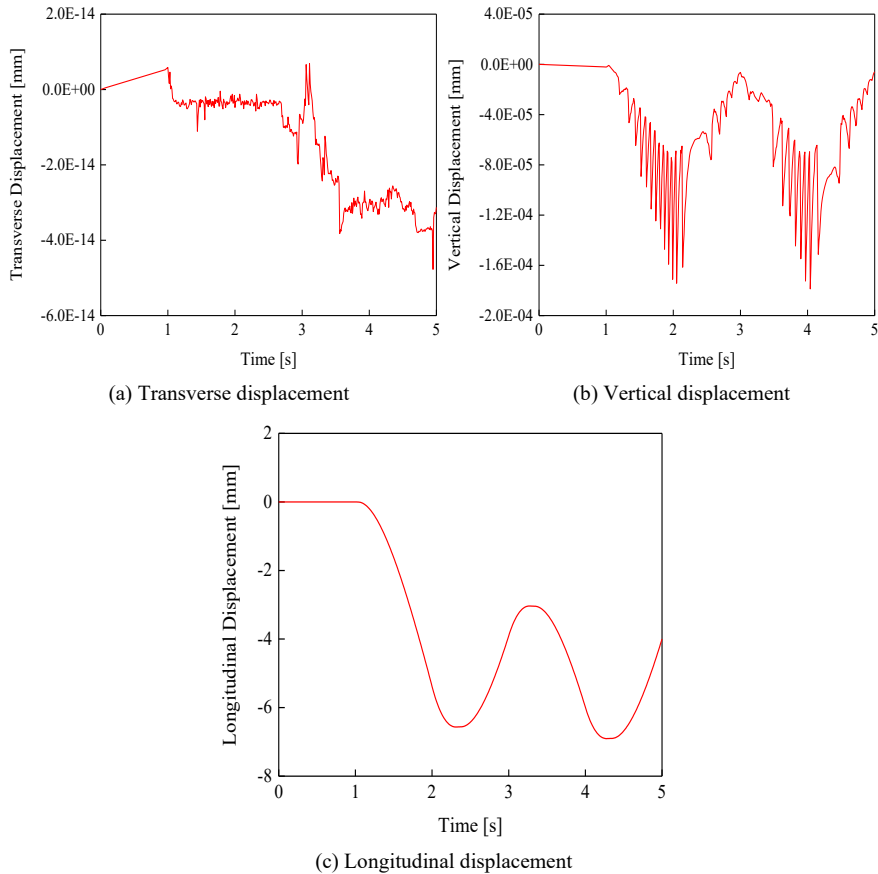


Figure 16

Response curves of slider displacements with the slider longitudinal tensile stress considered

Combined with Figs. 15~16, it can be identified that the reason for the slider-plate friction contact system to maintain the stick-slip vibration is the existence of increasing-decreasing cyclic variations in the slider motion velocity, i.e., there is a non-monotonic variation in the relative velocity of the contact interface, as shown in Fig. 17. In Fig. 17, the interval where the longitudinal velocity is zero is the adhesion phase, and the interval where the longitudinal velocity is non-zero is the slip phase. Therefore, the occurrence mechanism of the stick-slip vibration can be summarized as the presence of the non-monotonic variation of the relative velocity at the contact interface induces the formation of the stick-slip vibration.

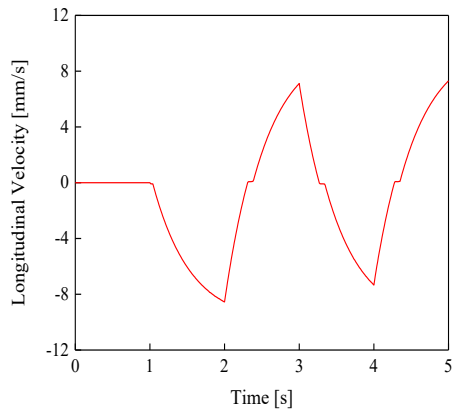


Figure 17

Slider longitudinal velocity curve with the slider longitudinal tensile stress considered

5 Behavior Characterization of Stick-Slip Vibration

In this section, the effects of different parameters on the stick-slip vibration behavior of the system will be mainly analyzed, so as to understand the stick-slip behavior and realize the effective control of stick-slip vibration.

5.1 Effect of Spring Stiffness

Based on the numerical model in Section 2, the spring stiffnesses are set to be 5 N/mm and 10 N/mm, respectively, and a constant velocity in the $-z$ direction is applied to the plate with an amplitude of 5 mm/s. By numerical calculations, the contact interface friction curves corresponding to different spring stiffnesses can be obtained, as shown in Fig. 18. It should be noted that the friction curves in Fig. 18 have been normalized for the purpose of comparison and are treated similarly below.

From Fig. 18, it can be seen that with the increase of time, the vibration phase of the friction force at the contact interface of the system with a spring stiffness of 5 N/mm will gradually lag behind that of the system with a spring stiffness of 10 N/mm, which indicates that the reduction of the spring stiffness slows down the stick-slip vibration degree of the system, thus decreasing the influence of stick-slip vibration on the system behavior.

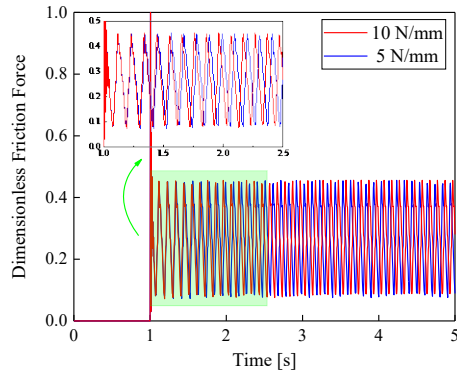


Figure 18
Friction force curves with different spring stiffnesses

5.2 Effect of Damper Damping

The spring stiffness in the numerical model is set to be 10 N/mm, and the damper damping takes the values of 5 Ns/mm and 10 Ns/mm, respectively, and the other conditions are kept consistent with the numerical model in Section 5.1. By calculation, the friction force curves of the contact interface under different damper damping conditions can be obtained, as shown in Fig. 19.

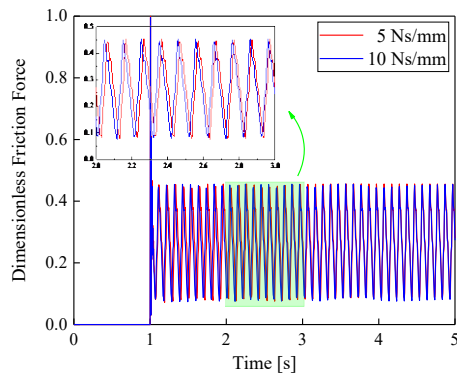


Figure 19
Friction force curves with different damper damping conditions

According to Fig. 19, it can be obtained that with the increase of time, the vibration phase of the friction force corresponding to a damper damping of 10 Ns/mm will gradually lag behind that corresponding to a damper damping of 5 Ns/mm, indicating that the increase of the damper damping will slow down the degree of stick-slip vibration of the system and reduce the system response caused by stick-slip vibration.

5.3 Effect of Friction Characteristic

The spring stiffness in the model is set to be 10 N/mm, and the friction characteristics are expressed using an exponential decay function (see Fig. 1) and a constant (0.35), respectively, and the other conditions are the same as in the numerical model of Section 5.1. The calculated friction force curves at the contact interface for different friction characteristic conditions are shown in Fig. 20.

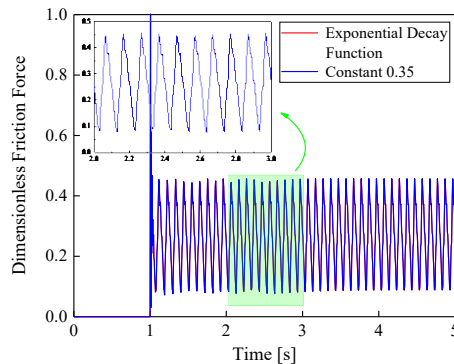


Figure 20

Friction force curves with different friction characteristics

From Fig. 20, it is easy to see that the friction force curves at the contact interface under different friction characteristics almost coincide throughout the time history, which illustrates that the exponential decay friction characteristic shown in Fig. 1 do not have a significant effect on the degree of stick-slip vibration of the system, as compared with the constant friction characteristic.

5.4 Effect of Motion Velocity

Similarly, the spring stiffness in the model is set to be 10 N/mm, and the plate has constant velocities in the $-z$ direction with amplitudes of 5 mm/s and 10 mm/s, respectively, to simulate different relative velocities at the contact interface, and the other conditions are consistent with the numerical model in Section 5.1. By calculation, the friction force curves at the contact interface corresponding to different plate motion velocities can be obtained, as shown in Fig. 21.

From Fig. 21, it can be seen that compared with the stick-slip vibration curve of the system contact interface corresponding to the plate motion velocity of 5 mm/s, the stick-slip vibration curve of the system contact interface corresponding to the plate motion velocity of 10 mm/s is more intensive in the time interval of 1~5 s, which demonstrates that the increase of the plate motion velocity will exacerbate the degree of stick-slip vibration of the system, thus further aggravating the dynamic response of the system.

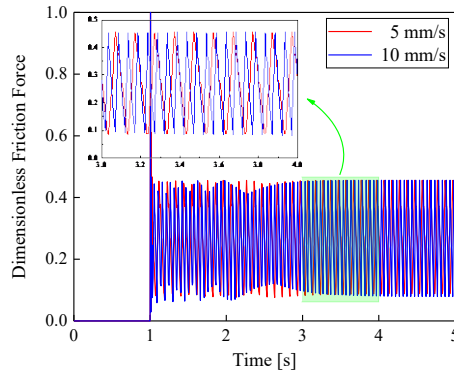


Figure 21

Friction force curves with different motion velocities

Conclusions

By using a three-dimensional finite element model of the slider-plate friction contact, the mechanism characteristics of the stick-slip phenomenon are analyzed in this paper in terms of both contact stick-slip and vibration responses, including slip vibration and stick-slip vibration. Meanwhile, the stick-slip vibration behavior of the system under the influence of different parameters, involving spring stiffness, damper damping, friction characteristics and plate motion velocity, is investigated. The main conclusions are as follows:

- (1) Depending on the vibration form of the system, the distribution and amplitude of contact stresses are not the same in the adhesion and slip states. In contrast to the frequency domain curve of the friction force for the slip vibration, the frequency domain curve of the friction force for the stick-slip vibration does not show a high-frequency component, suggesting that the high-frequency component of the friction force may be related to the sustained slip vibration.
- (2) The occurrence mechanism of the slip vibration is the presence and monotonic increment (or constancy) of the relative velocity at the contact interface leading to the formation of the slip vibration, whereas the occurrence mechanism of the stick-slip vibration is the presence of non-monotonic variation of the relative velocity at the contact interface leading to the formation of the stick-slip vibration.
- (3) The parametric analysis of stick-slip vibration shows that the reduction of spring stiffness, the increase of damper damping and the reduction of plate motion velocity will slow down the degree of stick-slip vibration of the system, thus decreasing the effect of stick-slip vibration on the system behavior. Compared to the constant friction characteristic of the contact interface, the exponential decay friction characteristic has less influence on the degree of stick-slip vibration of the system.

The novelty of this research lies in the fact, that the flexible body finite element model used can capture the contact state in detail and take into account the elastic deformation, which is beneficial for the comprehensive understanding of the stick-slip phenomenon.

Acknowledgements

The work presented in this research has partially been funded by the Shanghai Key Laboratory of Rail Infrastructure Durability and System Safety with project No. R202405. We thank the reviewers for their valuable comments and suggestions.

References

- [1] N. M. Kinkaid, O. M. O'Reilly, and P. Papadopoulos, "Automotive disc brake squeal," *J. Sound Vib.*, Vol. 267, No. 1, pp. 105-166, 2003, doi: 10.1016/S0022-460X(02)01573-0
- [2] J. Le Rouzic, A. Le Bot, J. Perret-Liaudet, M. Guibert, A. Rusanov, L. Douminge, F. Bretagnol, and D. Mazuyer, "Friction-induced vibration by Stribeck's law: application to wiper blade squeal noise," *Tribol. Lett.*, Vol. 49, No. 3, pp. 563-572, 2013, doi: 10.1007/s11249-012-0100-z
- [3] C. L. Dong, C. Q. Yuan, X. Q. Bai, X. P. Yan, and Z. Peng, "Tribological properties of aged nitrile butadiene rubber under dry sliding conditions," *Wear*, Vol. 322, pp. 226-237, 2015, doi: 10.1016/j.wear.2014.11.010
- [4] A. Meziane, L. Baillet, and B. Lualagnet, "Experimental and numerical investigation of friction-induced vibration of a beam-on-beam in contact with friction," *Appl. Acoust.*, Vol. 71, No. 9, pp. 843-853, 2010, doi: 10.1016/j.apacoust.2010.04.012
- [5] C. A. Brockley and P. L. Ko, "Quasi-harmonic friction-induced vibration," *J. Lubr. Technol.*, Vol. 92, No. 4, pp. 550-556, 1970, doi: 10.1115/1.3451469
- [6] R. A. Ibrahim, "Friction-induced vibration, chatter, squeal, and chaos—Part II: dynamics and modeling," *Appl. Mech. Rev.*, Vol. 47, No. 7, pp. 227-253, 1994, doi: 10.1115/1.3111080
- [7] K. Popp and P. Stelzer, "Stick-slip vibrations and chaos," *Philos. T. R. Soc. A*, Vol. 332, No. 1624, pp. 89-105, 1990
- [8] V. Utkin, "Variable structure systems with sliding modes," *IEEE T. Automat. Contr.*, Vol. 22, No. 2, pp. 212-222, 1977, doi: 10.1109/TAC.1977.1101446
- [9] K. Popp and M. Rudolph, "Vibration control to avoid stick-slip motion," *J. Vib. Control*, Vol. 10, No. 11, pp. 1585-1600, 2004, doi: 10.1177/1077546304042026

- [10] J. G. Hong, J. Kim, and J. Chung, "Stick-slip vibration of a moving oscillator on an axially flexible beam," *J. Mech. Sci. Technol.*, Vol. 34, No. 2, pp. 541-553, 2020, doi: 10.1007/s12206-020-0102-y
- [11] S. Maegawa, X. X. Liu, and F. Itoigawa, "Discussion of stick-slip dynamics of 2DOF sliding systems based on dynamic vibration absorbers analysis," *Lubricants*, Vol. 10, No. 6, p. 113, 2022, doi: 10.3390/lubricants10060113
- [12] M. Leus and M. Abrahamowicz, "Experimental investigations of elimination the stick-slip phenomenon in the presence of longitudinal tangential vibration," *Acta Mech. Automatica*, Vol. 13, No. 1, pp. 45-50, 2019, doi: 10.2478/ama-2019-0007
- [13] J. Abdo and R. Zaier, "A novel pin-on-disk machine for stick-slip measurements," *Mater. Manuf. Process.*, Vol. 27, No. 7, pp. 751-755, 2012, doi 10.1080/10426914.2011.648702
- [14] B. Balaram, B. Santhosh, and J. Awrejcewicz, "Frequency entrainment and suppression of stick-slip vibrations in a 3 DoF discontinuous disc brake model," *J. Sound Vib.*, Vol. 538, p. 117224, 2022, doi: 10.1016/j.jsv.2022.117224
- [15] C. L. Dong, J. L. Mo, C. Q. Yuan, X. Q. Bai, and T. Yu, "Vibration and noise behaviors during stick-slip friction," *Tribol. Lett.*, Vol. 67, No. 4, p. 103, 2019, doi: 10.1007/s11249-019-1216-1
- [16] H. Zhou, X. H. Long, and G. Meng, "Modeling for fretting behavior of nominally flat rough surfaces based on fractal theory," *J. Vib. Eng.*, Vol. 35, No. 4, pp. 895-902, 2022, doi: 10.16385/j.cnki.issn.1004-4523.2022.04.013
- [17] H. H. Qian, D. W. Wang, and J. L. Mo, "Effect of damping parameters on stability and stick-slip vibration behaviour of friction systems," *J. Vib. Meas. Diag.*, Vol. 41, No. 5, pp. 1021-1027+1040, 2021, doi: 10.16450/j.cnki.issn.1004-6801.2021.05.027
- [18] L. Wang, Y. L. Zhang, B.B. Tang, and Z. G. Li, "Analysis of stick-slip and chatter of the non-smooth vibration system with Dankowicz dynamic friction," *Chinese J. Appl. Mech.*, Vol. 35, No. 4, pp. 834-839+936, 2018, doi: 10.11776/cjam.35.04.C030
- [19] B. J. Song and S. Z. Yan, "Research progresses on interfacial stick-slip frictions," *China Mech. Eng.*, Vol. 28, No. 13, pp. 1513-1522, 2017, doi: 10.3969/j.issn.1004-132X.2017.13.001
- [20] S. Michael, *Abaqus/standard user's manual, version 6.14*. Providence, RI, Dassault Systèmes Simulia Corp, 2014
- [21] X. Z. Lu, C. W. Kim, and K. C. Chang, "Finite element analysis framework for dynamic vehicle-bridge interaction system based on Abaqus," *Int. J.*

- Struct. Stab. Dy.*, Vol. 20, No. 3, p. 2050034, 2020, doi: 10.1142/S0219455420500340
- [22] J. X. Shi, D. Chopp, J. Lua, N. Sukumar, and T. Belytschko, "Abaqus implementation of extended finite element method using a level set representation for three-dimensional fatigue crack growth and life predictions," *Eng. Fract. Mech.*, Vol. 77, No. 14, pp. 2840-2863, 2010, doi: 10.1016/j.engfracmech.2010.06.009
- [23] Z. N. Liao, X. D. Shao, Q. H. Qiao, J. H. Cao, and X. N. Liu, "Static test and finite element simulation analysis of transverse bending of steel-ultra-high performance concrete composite slabs," *J. Zhejiang Univ. (Eng. Sci.)*, Vol. 52, No. 10, pp. 1954-1963, 2018, doi: 10.3785/j.issn.1008-973X.2018.10.015
- [24] O. Polach, "Creep forces in simulations of traction vehicles running on adhesion limit," *Wear*, Vol. 258, No. 7-8, pp. 992-1000, 2005, doi: 10.1016/j.wear.2004.03.046
- [25] H. Lee, "A comparison of longitudinal adhesion models and identification of the dominant adhesion parameter," *Vehicle Syst. Dyn.*, Vol. 58, No. 4, pp. 590-603, 2020, doi: 10.1080/00423114.2019.1592204
- [26] E. Vollebregt, K. Six, and O. Polach, "Challenges and progress in the understanding and modelling of the wheel-rail creep forces," *Vehicle Syst. Dyn.*, Vol. 59, No. 7, pp. 1026-1068, 2021, doi: 10.1080/00423114.2021.1912367
- [27] B. Y. An, P. Wang, Y. X. Xu, J. M. Xu, and R. Chen, "Study on wheel/rail creep curve based on POLACH's method," *J. Mech. Eng.*, Vol. 54, No. 4, pp. 124-131, 2018, doi: 10.3901/JME.2018.04.124
- [28] T. H. Ma, M. L. Wu, and C. Tian, "Anti-skid control based on adhesion force observer for train pneumatic braking," *J. Tongji Univ. (Nat. Sci.)*, Vol. 48, No. 11, pp. 1668-1675, 2020, doi: 10.11908/j.issn.0253-374x.20010